Optimization of the Energy Performance of Airflow Windows

Dirk Saelens, Ph.D. **Staf Roels, Ph.D.** **Hugo Hens, Ph.D.**
Member ASHRAE

ABSTRACT

This paper presents an energy performance assessment of airflow windows with a built-in roller blind integrated in a narrow office building. The paper focuses on the use of optimal solutions to improve the performance of airflow windows for typical Belgian climatic conditions. First, the influence of changing the airflow window settings—the control of the airflow rate and the recuperation of the exhaust air—is studied. Secondly, two airflow window properties are scrutinized: the U-factor of the outer glazing and the distribution of the airflow over the cavity. Finally, the influence of a good insulated inlet zone is demonstrated and the effect of the insulation of the return duct is highlighted. The results of the optimized airflow windows are compared against the results of non-optimized variants and against the results of traditional solutions, including high-performance glazing with interior or exterior shading device.

INTRODUCTION

The sensibility for environmentally friendly and energy-conscious building design urged the need to develop new facade technologies. In the search toward energy efficient and visually attractive facades, multiple-skin facades (MSFs) are regularly presented as being valuable solutions to follow the desires of modern architecture. MSFs (also known as active envelopes, second skin facades, twin-facades, etc.) consist of two panes separated by a cavity through which air flows. The driving force for the airflow is natural or mechanical ventilation. In the cavity, usually a shading device is provided. Generally, distinction is made between naturally and mechanically ventilated MSFs. Extensive literature on MSF typologies and examples can, for example be found in Compagno (1995), Lang (1998), Gertis (1999), Ziller (1999), Baker et al. (2000), Oesterle et al. (2001), Arons and Glicksman (2001), and Poirazis (2004).

In the literature, numerous papers describe how MSFs should work to improve the building's energy efficiency. As many variants exist, the principles to reduce the energy demand strongly depend on the chosen typology. Some authors sum up the working principles and ideas to improve the energy efficiency without providing calculation results or experiments (Lieb 2001; den Boer and Ham 2001). Gertis (1999) correctly points out that only few simulations have been made and that only few measurements are available to support the claimed benefits. Other researchers provide models to study the performance of specific MSF typologies. They, however, do not link the envelope level results to the building energy performance or do not couple the model to a building energy simulation program (Holmes 1994; Park et al. 1989; Tanimoto and Kimura 1997; Helbig 1999; Manz and Simmler 2003). Only few combinations of MSF modeling and building energy simulation are available. Most of these papers are restricted to only one MSF typology. Müller and Balowski (1983) analyze airflow windows, Oesterle et al. (2001) give a comprehensive survey of double-skin facades, and Haddad and Elmahdy (1998) discuss the behavior of supply air windows. Recent studies have recognized that an optimal control strategy combined with an overall building analysis is necessary to increase the energy efficiency of MSFs (Saelens 2002; Park 2003).

Dirk Saelens is a post-doctoral researcher, **Staf Roels** is an associate professor, and **Hugo Hens** is a professor and head of the Laboratory of Building Physics, K.U.Leuven, Leuven, Belgium.

In this paper, the energy demand of an office equipped with mechanically ventilated airflow windows (AFW) is discussed. The energy efficiency depends on several aspects of the AFW configuration. Distinction is made between parameters that can be changed—the system settings—and parameters that are fixed for a given typology—the system properties. Regarding the settings, the importance of a controllable airflow rate and an intelligent recuperation of the air returning from the AFW are shown. It is shown that traditional cladding systems are not necessarily outperformed by AFWs. As far as the properties are concerned, the position of the shading device and the U-factor and solar properties of the glazing are scrutinized. Finally, the importance of correctly designed connections between the office and the AFW inlet zone and between the AFW outlet and HVAC plant is analyzed. The influence of a good insulated inlet and outlet zone is demonstrated and the effect of the insulation of the return duct is highlighted.

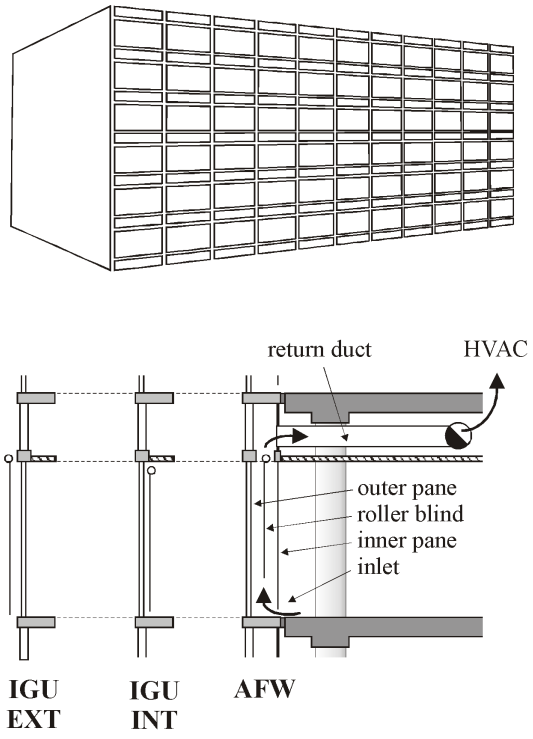

Figure 1 *Diagram of the simulation object: above, an impression of the office building; below, the layout of the different facade systems. IGU EXT is a traditional cladding solution with exterior shading device, IGU INT is a traditional cladding solution with interior shading device, and AFW is a mechanically ventilated airflow window. (Drawings are not to scale.)*

MODELING

Simulation Object

The annual energy simulation is based upon Belgian climatic conditions and is performed with a time step of a quarter of an hour. The investigated building is a narrow office building with offices along a central corridor. The six-story office building measures 44.0 × 13.2 × 18.0 m (144 × 43 × 59 ft) (width × depth × height). The individual offices measure 4.0 × 6.0 × 3.0 m (13.1 × 19.7 × 9.8 ft) (width by depth by height) and each is supposed to house two occupants. The main facades face north and south (Figure 1). The transparent surface measures 4.0 × 2.6 m (13.1 × 8.5 ft) (width × height). The airflow window (Figure 1: AFW) is equipped with an insulated glazing unit at the outside, an internal roller blind in the cavity, and a single glass at the inside. The material properties are listed in Table 1. The roller blind is lowered as soon as the solar radiation on the facade exceeds 75 W/m² (24 Btu/[h·ft²]). Obviously, this is not the optimal scenario. Optimal strategies have to balance between increasing the cooling load while lowering lighting, or vice-versa. Furthermore, occupants' comfort has to be ensured; glare should be avoided while a clear view is appreciated. These aspects were not considered in the presented study. The opaque part at the outlet zone measures 4.0 × 0.6 m (13.1 × 2.0 ft) (width × height) and consists of an insulated cladding system (properties: Table 1). The airflow window is ventilated with interior air. The minimal airflow rate through the AFW equals 30 m³/(h·m) (70 cfm/ft). In such a way, the total airflow rate through the base case AFWs equals the total ventilation requirements of the building. The base case variant assumes that the air is evenly

Table 1. Fenestration Properties

	Description	U-Factor W/(m²·K) (Btu/[h·ft²·°F])		g-Value (SHGC) (-)
insulated glazing unit	low-emission glass, argon filled	1.23 (0.22)		0.59
single glass	normal clear float glass	5.67 (1.00)		0.85
cladding	insulated cladding system	0.58 (0.10)		–
		transmission	**reflection**	**absorption**
shading device	roller blind	0.08	0.09	0.83

Table 2. Sensible Internal Gains (SI units)

	Value	Total	Radiative Part	Convective Part
occupancy	75 W/person	150 W	50%	50%
lighting	5 W/m²	120 W	10%	90%
appliances	125 W/person	250 W	30%	70%
occupancy	256 Btu/(h·person)	512 Btu/h	50%	50%
lighting	1.6 Btu/(h·ft²)	409 Btu/h	10%	90%
appliances	426 Btu/(h·person)	853 Btu/h	30%	70%

distributed over both cavities when the shading device is lowered. Hence, the fraction of the airflow through the outer cavity F_{ex} = 0.5. The airflow window system is part of the return path to the HVAC system (Figure 1). First, the air flows through an inlet zone, passes the airflow window, is then collected in the outlet plenum, and flows back to the HVAC plant through the return duct in the false ceiling. The results of the AFW are compared against two traditional solutions: an insulated glazing unit with interior shading device (Figure 1: IGU INT) and an insulated glazing unit with exterior shading device (Figure 1: IGU EXT).

The setpoint temperature for heating is 21°C (70°F), with a night setback to 16°C (61°F). The setpoint temperature for cooling is 26°C (79°F). Cooling is only allowed during office hours (from 7 a.m. to 7 p.m.). The heating and cooling controllers have a dead band temperature of 1 K. Internal gains due to occupancy, lighting, and office appliances are summarized in Table 2. The internal gains are split into a convective and radiative part according to the ASHRAE guidelines (ASHRAE 1997). The convective gains are added to the air temperature; the radiative gains are distributed over the internal surfaces proportional to the surface area. As the office is situated next to a large glazed surface, the internal gains due to lighting are assumed small.

In the analysis, the load or energy demand of the office is presented as an average per unit of office floor. It is defined as the energy needed to keep the office temperature between the setpoints. The energy demand includes the ventilation energy, control inefficiencies, and distribution losses of the air ducts, but it excludes the energy needed to power the fans, nor does it take into account the efficiency of the HVAC plant.

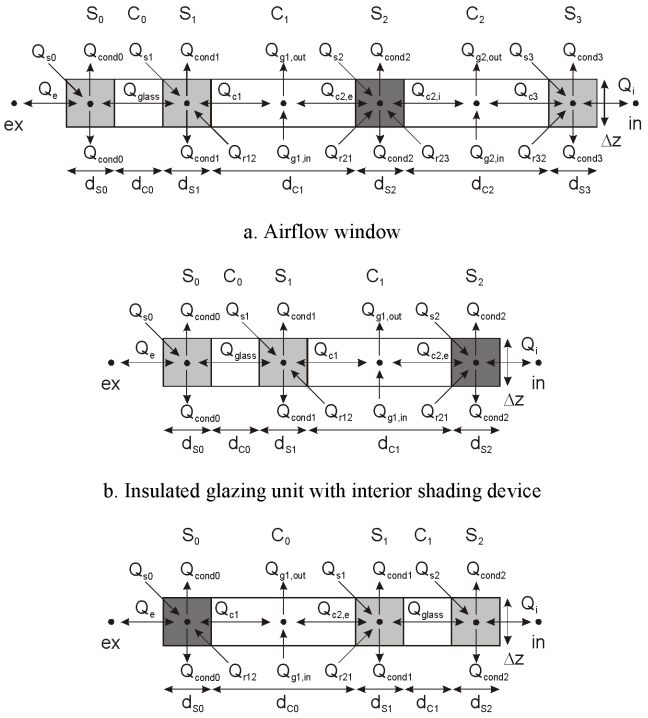

Figure 2 *Diagram of a horizontal layer of the numerical model for the (a) airflow window and (b and c) the insulated glazing units. (Legend:* S = *surface;* C = *cavity;* Q_s = *direct solar energy;* Q_{cond} = *conduction heat flux;* Q_g = *enthalpy flow;* Q_c = *convective heat flux;* Q_r = *radiant environment;* Q_i = *heat exchange with internal environment.)*

Facade Models

In this study, the thermal behavior of the AFW is calculated with a cell-centered finite volume method (Saelens 2002). The AFW is divided into four or six vertical layers (depending on the position of the roller blind: raised or lowered) (Figure 2a), which are, in turn, divided into 32 parts along the height. For each volume, the heat balance is written. At the cavity surfaces (S1, S2, and S3), three heat transfer modes are taken into account: conduction (Q_{cond}), convection (Q_c), and radiation (Q_r). The convective heat transfer (Q_{conv}) in the presented model depends on the airflow rate and the temperature difference between the surface and the air. Radiant heat transfer (Q_r) for each surface is calculated with the net-radiation method (Siegel and Howell 1992). In the cavities (C1 and C2), the heat transfer is governed by convection and enthalpy transport due to the airflow. Heat transfer between the two panes of the double glazing (Q_{glass}) is a combination of conduction, convection, and radiation and is calculated

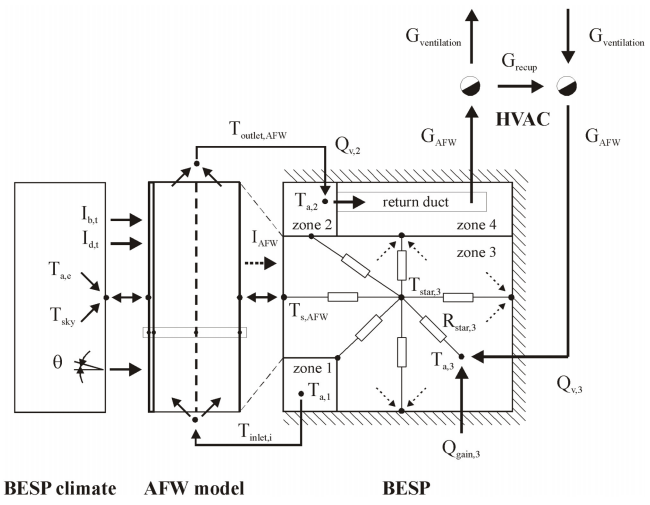

Figure 3 *Implementation of the numerical model in the energy simulation program in case of the airflow window.*

using manufacturers' data. The absorbed solar energy (Q_s) is calculated for each separate layer with an embedded technique described by Edwards (1977). It is a function of the angle of incidence and also accounts for partial shading of the panes. The heat transfer with the surroundings (Q_e and Q_i) is described with a combined heat transfer coefficient. Long-wave radiation at the outside is taken into account by using a sky temperature. Finally, it is assumed that the roller blind, when lowered, perfectly obstructs air exchange between both cavities. This assumption was confirmed by measurements (Saelens 2002) and CFD simulations (Janssens 2003). The airflow rate in the mechanical flow variant is a known variable and, hence, the thermal system can be solved easily. The validation of the presented model is described in Saelens (2002).

A similar model is also used to calculate the thermal behavior of the traditional solutions (IGUs). When the shading device is lowered, a naturally ventilated cavity is formed between the glazing and the roller blind. The cavity of the variant with interior shading device is ventilated with interior air (Figure 2b). That of the variant with exterior shading device is ventilated with exterior air (Figure 2c). As the airflow rate and the temperature profiles in the naturally ventilated cavity of these traditional solutions are mutually dependent, an iterative solution method to solve the thermal system is used.

Implementation

The AFW model is coupled to TRNSYS, a commercially available dynamic building energy simulation program (BESP). The AFW-model passes the inner pane average surface temperature ($T_{s,AFW}$), the cavity exhaust air temperature ($T_{outlet,AFW}$), and the total transmitted solar energy (I_{AFW}) to the BESP. The simulation program, in turn, provides the AFW model with the incident direct ($I_{b,t}$) and diffuse ($I_{d,t}$) solar radiation, the angle of solar incidence (θ), the zone air ($T_{a,3}$) and average surface temperature (part of T_{star}), the exterior air ($T_{a,e}$) and sky temperature (T_{sky}), and the cavity air inlet temperature ($T_{a,1} = T_{inlet,1}$) (Figure 3). As the results of both programs are mutually dependent, an iteration between the AFW model and the BESP is carried out until convergence is achieved.

In the case of the traditional solutions, the inlet and outlet zones are not ventilated. The implementation of the surface temperature and the incoming solar radiation remains the same. When the shading is lowered, the interior or exterior temperature acts as inlet temperature for the cavity. In the case of the traditional solution with interior shading device, there is an extra heat source when the shading device is lowered: the heated air from the cavity is added to the convective term into the office zone ($Q_{gain,3}$).

ENERGY DEMAND ANALYSIS

System Settings

Energy efficiency is a commonly stated argument for choosing AFWs as a facade concept. Two main principles can be distinguished: (1) AFWs may reduce the transmission losses in winter and the transmission gains in summer and (2) AFWs can either reuse the return air in order to use the collected solar energy or recover some of the transmission losses or expel the return air to avoid overheating and to remove the absorbed solar radiation.

The effect of these principles is first analyzed for the base case AFWs. To optimize the energy efficiency, two control mechanisms are added to the base case variants (Table 3). These three AFW variants are also compared against the results of traditional solutions.

Base Case Results. Figure 4 compares the energy demand of the AFW with the traditional solutions. Let us first analyze the base case results. Although the traditional solutions (Figure 4a, IGU EXT and IGU INT) have higher transmission losses than the AFW, the heating demand of these solutions is not outperformed by the base case AFW (Figure 4a, AFW). This can be attributed to the difference in direct solar gains. Because of the extra pane and shading, the direct solar gains of the AFW are smaller than those of the IGUs. For the studied configuration, both effects almost compensate. The most energy-consuming solution (Figure 4a, IGU EXT) requires only somewhat more heating energy than the AFW (Figure 4a, AFW). The traditional variant with interior shading device (Figure 4a, IGU INT) performs somewhat better because of the higher indirect solar gains. The difference between the minimum and maximum cooling load is more pronounced (Figure 4b, AFW, IGU INT, and IGU EXT). Again, the traditional solutions are not necessarily outperformed. The results show that the cooling energy is determined by the indirect solar gains. Despite the higher direct solar gains, the IGU with exterior shading device requires 21%

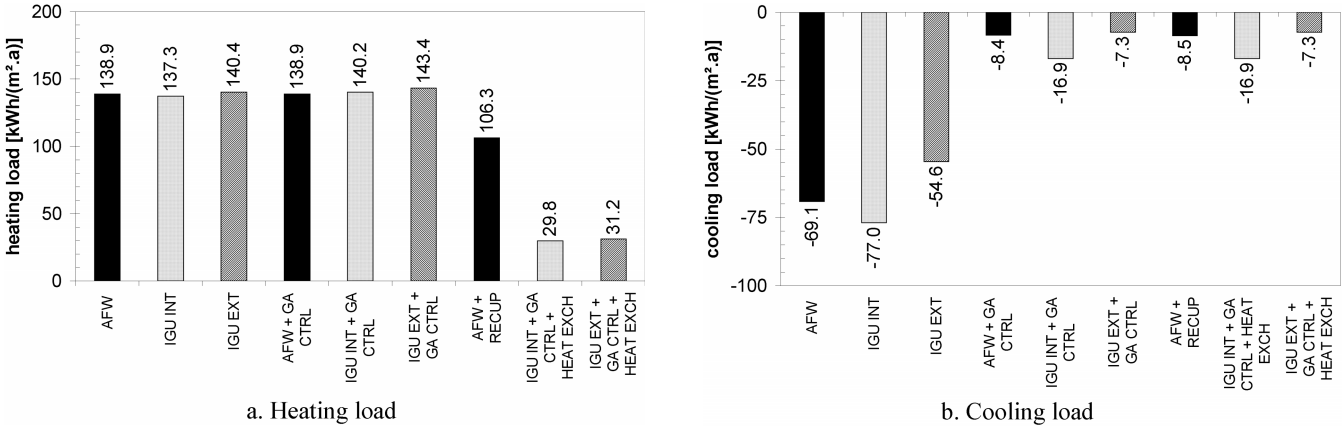

Figure 4 *Annual heating and cooling load per unit of floor area. (Legend: see Table 3.)*

Table 3. Studied Variants

Variant	Acronym	Description
Multiple-Skin Variants		
base case	AFW	The airflow rate through the AFWs equals the total ventilation airflow rate. No airflow rate control strategies are applied and the return air cannot be recovered.
airflow rate control	AFW + GA CTRL	Previous calculations (Saelens 2002) have indicated that a variable airflow rate may improve both the cooling and heating load. During heating demand, a low airflow rate is favorable. During cooling demand, an increase of the airflow rate helps to lower the cavity temperature. According to the climatic conditions and the energy demand, the airflow rate can double. The system is able to control both orientations separately.
recuperation of the exhaust air	AFW + RECUP	When the return temperature is higher than the interior temperature, the air returning to the HVAC plant can be reused to lower the heating demand. To be able to reuse air, the total airflow rate should be higher than the ventilation airflow rate. Therefore, this system is combined with the airflow rate control system. Whenever appropriate, the system increases the airflow rate through the AFW to be able to reuse part of the return air. As for the previous variant, the system tries to lower the cooling load by increasing the airflow rate.
Traditional Variants		
base case	IGU INT	Traditional glazing with interior shading device. The office is ventilated with the same airflow rate as in the AFW base case. No airflow rate control strategies are applied and the return air cannot be recovered.
	IGU EXT	As in the previous case (IGU INT) but with exterior shading device.
airflow rate control	IGU INT + GA CTRL	Traditional glazing with interior shading device and airflow rate control. During heating demand, a low airflow rate is chosen to lower the ventilation energy. During cooling demand, an increase of the airflow rate cools down the building as long as the exterior temperature is lower than the interior temperature.
	IGU EXT + GA CTRL	As in the previous case (IGU INT + GA CTRL) but with exterior shading device.
heat exchanger	IGU INT + GA CTRL + HEAT EXCH	Traditional glazing with interior shading device and airflow rate control. On the exhaust of the HVAC plant, a cross-flow heat exchanger system is used to recover part of the ventilation energy.
	IGU EXT + GA CTRL + HEAT EXCH	As in the previous case (IGU INT + GA CTRL + HEAT EXCH) but with exterior shading device.

less cooling energy than the AFW (Figure 4b, IGU EXT). The IGU with interior shading device suffers from the high indirect solar gains and needs 11% more cooling energy than the AFW, turning it into the worst choice to control the cooling load.

Airflow Rates Control Results. As long as the airflow rate does not exceed the total ventilation rate of the building, an increase of the cavity airflow rate is favorable to lower the heating demand (Saelens 2002). It increases the cavity temperature and reduces the transmission losses. In such a way, AFWs are used as a heat exchanger for the exhaust air. If recuperation of air is impossible, extra exterior air has to be inserted into the building as soon as the total AFW airflow rate exceeds the total ventilation rate of the building. The heating of this extra ventilation air has a higher energy cost than the reduction of the transmission losses (Saelens 2002). Consequently, the airflow rate based on the ventilation rate is the most favorable option to reduce the heating demand. As a result, the airflow rate controller chooses the minimal ventilation rate, and the heating demand does not change compared to the base case AFW (Figure 4a, AFW and AFW + GA CTRL). In summer, an increase of the airflow rate helps to lower the cooling load with an astonishing 88% (Figure 4a, AFW and AFW + GA CTRL). Two effects are important: (1) the reduction of the indirect solar gains due to the increased airflow in the AFW and (2) the free cooling effect by increasing the exterior ventilation. Closer analysis of the results shows that the latter is far more important. Obviously, the same strategy can be applied to lower the cooling demand of the traditional solutions as well. As for the AFWs, the cooling needs of the traditional solutions drop significantly if an airflow rate controller is used (Figure 4b, IGU EXT GA and IGU INT GA). The cooling needs of the traditional exterior shading device with airflow rate control (Figure 4b, IGU EXT GA) prooves to be the lowest. If an exterior shading device is impossible or unwanted, the airflow window is a valuable alternative for insulated glazing units with interior shading. It should be noted that an increase of the airflow rate causes a higher fan consumption. This has to be taken into account in an overall energy consumption analysis but is not included in this study.

Recuperation of Exhaust Air Results. As a further step to save heating energy, recuperation of the return air is implemented. The recuperation path (G_{recup}) is indicated in Figure 3. Only when the total airflow rate exceeds the required ventilation airflow rate is recuperation of the AFW return air possible; therefore, this strategy is implemented as an addition to the airflow rate control system. In order to save energy, the return temperature in the HVAC plant should be higher than the interior temperature. In this analysis, the system increases the airflow rate if heating is needed and the outlet temperature is warmer than the setpoint temperature for heating. As the north and south facade have a different thermal behavior, the system is able to control both orientations separately. When the outlet temperature drops below the setpoint temperature for heating, the airflow rate is set back to the minimal ventilation airflow rate and recuperation is no longer possible. The results (Figure 4a, AFW + RECUP) show that it is useful to implement this strategy to decrease the heating load while the cooling load is only marginally increased (Figure 4b, AFW + RECUP). A heating demand reduction of 24% is possible, but, again, a raise in fan consumption has to be paid.

As an alternative for the traditional solutions, a crossflow heat exchanger system on the exhaust of the HVAC plant is analyzed. The results (Figure 4a, IGU INT HE + GA and IGU EXT HE + GA) show that this method is very efficient to reduce the heating demand. The cooling demand is not changed if the heat exchanger can be bypassed (Figure 4b, IGU INT HE + GA and IGU EXT HE + GA). Obviously, heat exchangers can also be applied in combination with AFWs.

System Properties

As shown above, the energy efficiency of AFWs is significantly determined by a correct setting of the system parameters. Choosing correct properties of the materials used to build the AFW and optimizing some geometrical aspects of the facade layout may further improve the energy efficiency of AFWs. In this section, the influence of the U-factor and solar properties of the glazing and the position of the shading device in the cavity are studied.

U-Factor. Figure 5 shows the relative influence of replacing the exterior pane of the AFW with glazings with a higher U-factor (U-factor = 2.10 W/[m²·K] [0.37 Btu/(h·ft²·°F)] and U-factor = 3.00 W/[m²·K] [0.53 Btu/(h·ft²·°F)]) compared to the AFW variant with the same control strategy and a U-factor = 1.23 W/m²K (0.22 Btu/[h·ft²·°F]). Table 4 summarizes the properties of the IGUs. Commonly, low-E coatings are used to improve the thermal insulation quality of the glazing. As a consequence, the solar properties are also closely related to the U-factor. Because the IGUs with higher U-factor do not have a low-E coating, their g-value (the g-value equals the solar heat gain coefficient [SHGC]) is significantly higher. On the one hand, the IGUs with higher U-factor increase the direct solar gains. On the other hand, the lower thermal resistance of these glazings enhances the cooling of the air flowing through the cavity. The resulting heating demands (Figure 5a) show that the latter effect is slightly dominant: the heating demand increases if we replace the exterior IGU by a less insulating type. The difference is more pronounced when we allow recuperation (Figure 5a, AFW + RECUP). In this case, the return air is to be reused in the HVAC plant, and the cooling effect of the IGU with U-factor = 3.00 W/(m²·K) (0.53 Btu/[h·ft²·°F]) is emphasized more. The increase of the direct solar radiation determines the cooling results: the IGU with the lowest g-value performs best. The differences between the IGU with the same g-value are a result of the insulation quality. The cooling demand is lower if the air flowing through the cavity cools down more. As a result, the cooling demand of the IGU with U-factor = 2.10 W/(m².K) (0.37 Btu/[h·ft²·°F]) is higher than that with a U-factor of 3.00 W/(m².K) (0.53 Btu/[h·ft²·°F]) (Figure 5b).

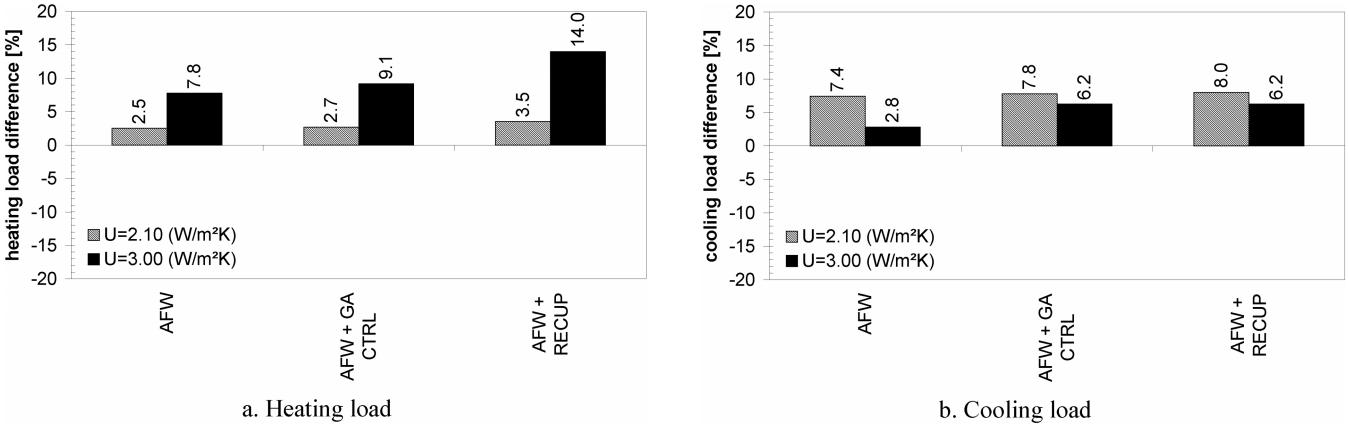

Figure 5 *Annual heating and cooling load per unit of floor area as a function of the exterior glazing U-factor. The results are relative to the base case AFW-variant in Figure 4 with the same control strategy. (Legend: see Table 3.)*

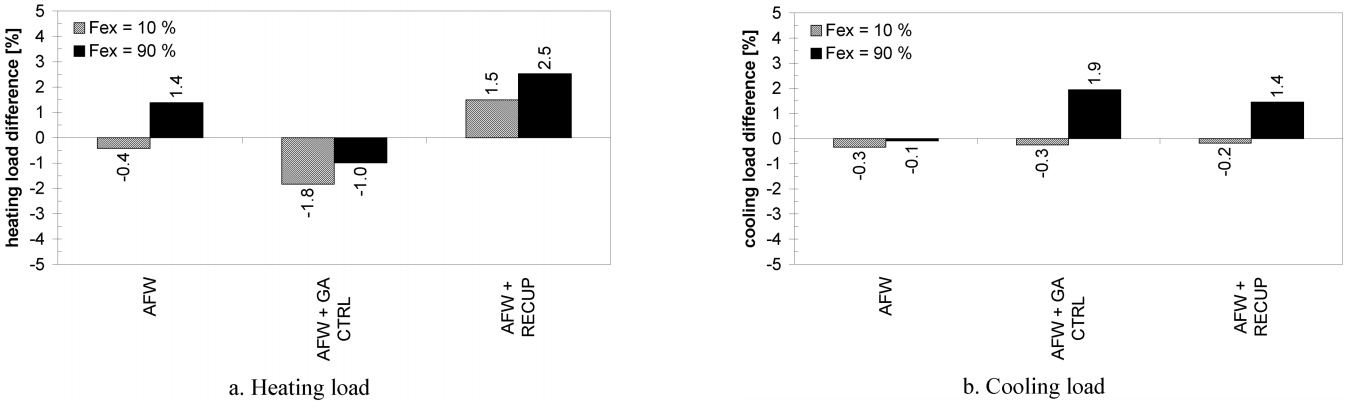

Figure 6 *Annual heating and cooling load per unit of floor area as a function of the airflow distribution through the exterior cavity (F_{ex}). The results are relative to the base case AFW-variant in Figure 4 with the same control strategy. (Legend: see Table 3.)*

Table 4. IGU Glazing Properties

Glazing Type	U-Factor (W/[m²·K])	U-Factor Btu/(h·ft²·°F)	g-Value (SHGC) (-)	Description
IGU 1	1.23	0.22	0.59	low-E coating, argon-filled glazing
IGU 2	2.10	0.37	0.76	argon-filled glazing
IGU 3	3.00	0.53	0.76	standard double glazing

Shading Device Position. The position of the shading device determines the fraction of the air flowing through the outer and inner cavity. Janssens (2003) shows that for a roller blind, the fraction is proportional to the third power of the cavity thickness. The distribution of the airflow over the inner and outer cavity influences the surface temperature of the inner pane and the outlet temperature. On the one hand, the inner cavity heats up more if it is not properly ventilated. As a result, the inner surface temperature is higher when the airflow rate through the outer cavity is higher. This lowers the heating demand but increases the need for cooling. On the other hand, the outlet temperature at the top of the cavity decreases when the fraction of air flowing through the outer facade increases. This reduces the heating and cooling demand. As a consequence, the overall results are difficult to interpret. Figure 6 shows the relative difference for the heating and cooling load as a function of the airflow fraction through the outer cavity (F_{ex}). All in all, the differences are relatively

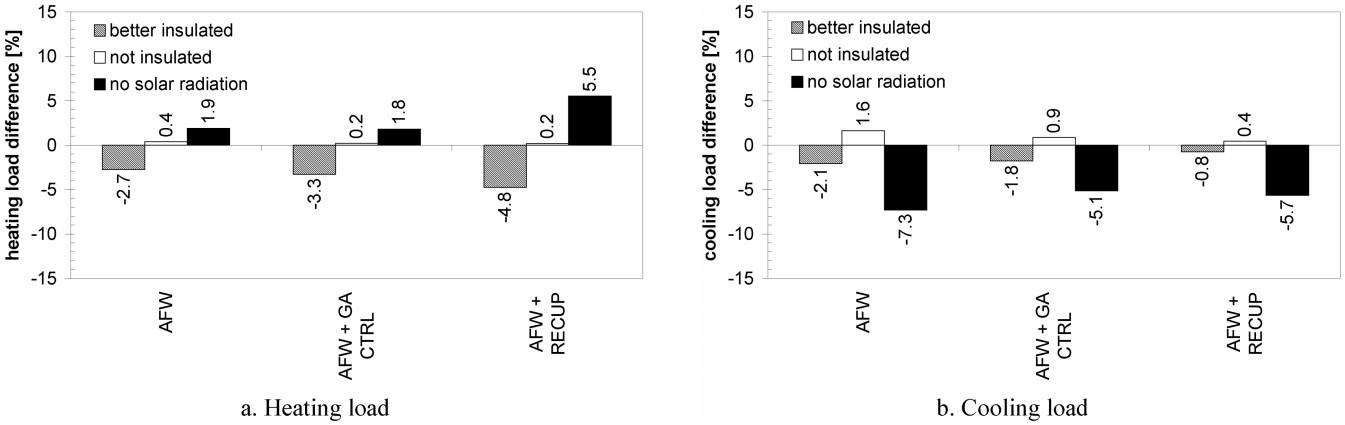

Figure 7 *Annual heating and cooling load per unit of floor area as a function of the insulation quality and the solar radiation in the inlet zone. The results are relative to the base case AFW-variant in Figure 4 with the same control strategy. (Legend: see Table 3.)*

small. However, from a thermal comfort point of view, lower surface temperatures are favorable to avoid asymmetrical radiation in summer. The surface temperature may exceed 45°C (113°F). Therefore, a shading device closer to the exterior facade is suggested, as it enhances the airflow through the inner facade.

Implementation

The connections of the AFW with the interior and the return duct require special attention, not only from a construction point of view—construction beams may, for example, obstruct an easy connection with the return duct—but also from an energy point of view. In this section, the importance of correctly designed connections between the office and the AFW inlet zone and between the AFW outlet and HVAC plant is analyzed.

Inlet Zone. Measurements illustrate that the assumption of an inlet temperature equal to the interior air temperature is usually not valid (Saelens et al. 2004). The inlet temperature is influenced by the transmission losses and gains through the outer and inner bounding surfaces and by the solar radiation in the inlet zone. Calculating the inlet temperature by assuming the inlet zone as a separate zone in the energy simulation program proved to be capable of reproducing the measured inlet temperatures (Saelens et al. 2004). The same simulation approach is used here (Figure 3). Three cases are analyzed: (1) the thermal insulation of the inlet zone is increased by using exterior profiles with a better thermal break (Figure 7: better insulated), (2) the thermal insulation of the inlet zone is decreased by using aluminum profiles without thermal break and (Figure 7: not insulated), and (3) solar radiation in the inlet zone is ignored (Figure 7: no solar radiation). The properties of the different cases are summarized in Table 5. Figure 7 illustrates the change of the heating and cooling demand relative to the AFW variant with the same control strategy. A higher insulation level of the inlet zone increases the inlet temperature in winter. This results in a higher overall temperature of the AFW and, as a consequence, the heating demand decreases. Not insulating the inlet zone results in a higher heating demand and increases the risk of condensation in the cavity inlet zone. In summer, the heating of the exterior surface becomes important. A better insulation prevents excessive heating of the inlet zone. Ignoring the solar radiation results in an underestimation of the inlet temperature and an overestimation of the heating load. Also the solar radiation has an important influence on the cooling load. Not accounting for the heating due to solar radiation may lead to an important underestimation of the cooling demand. The results suggest benefits may be obtained by avoiding excessive absorption of solar radiation. This can be achieved by choosing highly reflective finishings.

Plenum. The air returning from the AFW is collected in the outlet zone, which is, in turn, connected to an exhaust duct to the HVAC plant. The return duct is running through the false ceiling space (Figure 3). As the return air is no longer at interior temperature, it causes gains or losses in the false ceiling. Two cases are analyzed: (1) the insulation of the false ceiling is increased by doubling the insulation thickness (Figure 8: better insulated) and (2) the return duct and false ceiling are not insulated (Figure 8: not insulated). The properties of the different cases are summarized in Table 5. Figure 8 shows the considerable influence of the insulation quality of the return duct and the false ceiling. In winter, the average return air is colder than the interior air. On average, the plenum will be somewhat colder than the office and, consequently, the heating demand decreases with increasing insulation (Figure 8a, AFW). When the return air is to be reused in the case of the variant with recuperation (Figure 8a, AFW + RECUP), the

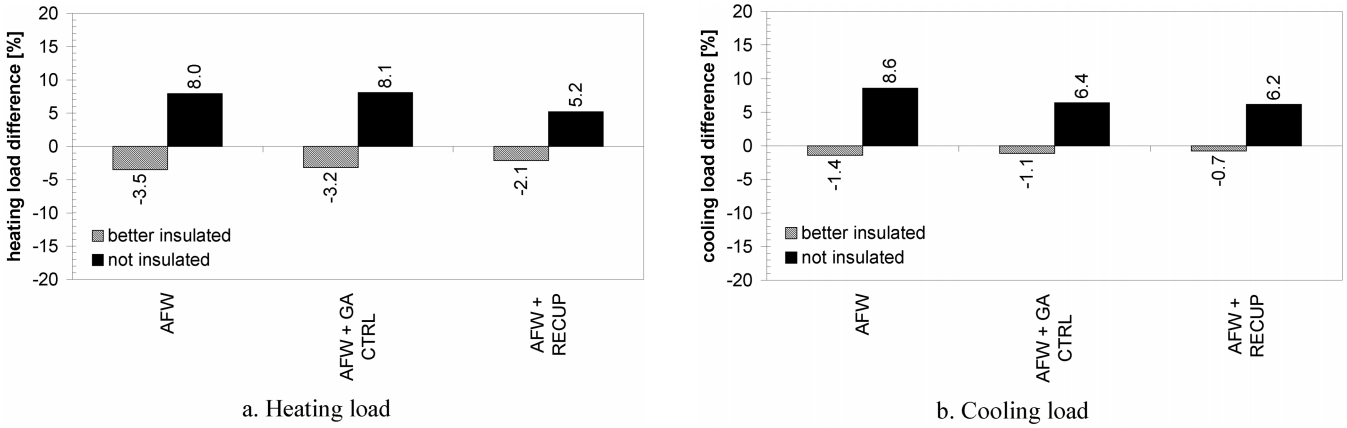

Figure 8 *Annual heating and cooling load per unit of floor area as a function of the insulation quality of the return duct and false ceiling. The results are relative to the base case AFW-variant in Figure 4 with the same control strategy. (Legend: see Table 3.)*

Table 5. Description of the Cases in the Implementation Study

Position	Case	Description and Properties
	base case	average U-factor inlet zone: U = 1.1 W/(m²·K) (0.19 Btu/[h·ft²·°F]) thermal resistance return duct: R = 1.5 m²·K/W (8.5 h·ft²·°F/Btu) thermal resistance ceiling: R = 1.6 m²·K/W (9.1 h·ft²·°F/Btu) heating due to solar radiation in the inlet zone is accounted for
inlet	better insulated	as in base case but: average U-factor inlet zone: U = 0.5 W/(m²·K) (0.09 Btu/[h·ft²·°F])
	not insulated	as in base case but: average U-factor inlet zone: U = 1.7 W/(m²·K) (0.30 Btu/[h·ft²·°F])
	no solar radiation	as in base case but: heating due to solar radiation in the inlet zone is not accounted for
plenum	better insulated	as in base case but: thermal resistance return duct: R = 1.5 m²·K/W (8.5 h·ft²·°F/Btu) thermal resistance ceiling: R = 2.9 m²·K/W (16.5 h·ft²·°F/Btu)
	not insulated	as in base case but: thermal resistance return duct: R = 0.2 m²·K/W (1.1 h·ft²·°F/Btu) thermal resistance ceiling: R = 0.3 m²·K/W (1.7 h·ft²·°F/Btu)

situation becomes more difficult. During sunny winter days, the return air is warmer than the interior air. A lower insulation level increases the gains from the return duct but lowers the return temperature at the HVAC plant. The former phenomenon is more important and suggests that a lower insulation level is favorable. However, during the time the AFW-outlet temperature is lower than the interior, a better insulation is beneficial. This is the reason why the difference between "insulated" and "not insulated" only becomes negligible and does not reverse. In summer, the average return air temperature is higher than the interior air. The air flowing through the return duct increases the solar gains in the office. As a result, the cooling load increases if the return duct is less insulated (Figure 8b, AFW). If the airflow rate control is switched on to lower the cooling demand (Figure 8b, AFW + GA CTRL and AFW + RECUP), the AFW-outlet temperature is lower. As a result, the difference in cooling demand between the different solutions becomes negligible.

CONCLUSIONS

In this paper, different strategies to optimize the energy efficiency of airflow windows were studied and compared with the results of traditional cladding systems. The energy efficiency of airflow windows is significantly determined by

an optimal control of the system settings and a correct choice of the system properties.

Regarding the settings, the importance of a controllable airflow rate to reduce the cooling load and an intelligent recuperation system to recover part of the air returning from the airflow window to reduce the heating demand is shown. Nevertheless, traditional solutions are not necessarily outperformed.

Regarding the airflow window properties, the U-factor and solar properties of the glazing and the position of the shading device are scrutinized. The glazing with the lowest U-factor and lowest solar transmittance proved to be a good choice to lower both heating and cooling demand. The airflow rate distribution has only a small impact on the energy demand. A good ventilation of the inner cavity is beneficial to improve thermal comfort near the facade.

Finally, the importance of correctly designed connections between the office and the airflow window inlet zone and between the airflow window outlet and HVAC plant was demonstrated. To achieve optimal energy efficiency, the inlet zone must be well insulated and reflect solar radiation. Furthermore, the return duct should be well insulated. In winter, the cold return air prevents the office from cooling down. In summer, excessive gains from the warm return air are avoided.

ACKNOWLEDGMENTS

This research is funded by a research grant of the Flemish Institute for the Promotion of Industrial Scientific and Technological Research (IWT: Vlaams Instituut ter Bevordering en Promotie van het Wetenschappelijk-Technologisch Onderzoek in de Industrie). Their financial contribution is gratefully acknowledged.

REFERENCES

Arons, D.M.M., and L.R. Glicksman. 2001. Double skin, airflow facades: Will the popular European model work in the USA? *Proceedings of ICBEST 2001, International Conference on Building Envelope Systems and Technologies, Ottawa, Canada* 1:203-207.

ASHRAE. 1997. *1997 ASHRAE Handbook—Fundamentals*. Atlanta: American Society of Heating, Refrigerating and Air-Conditioning Engineers, Inc.

Baker, P., D. Saelens, M. Grace, and T. Inoue. 2000. Advanced Envelopes—Methodology, evaluation and design tools, Final report IEA Annex 32 (IBEPA), Leuven: Acco.

Compagno, A. 1995. *Intelligent Glass Facades—Material, Practice, Design*. Basel: Verlag für Architektur.

Edwards, D.K. 1977. Solar absorption by each element in an absorber-coverglass array. *Solar Energy* 19:401-402.

den Boer, T.L.J., and M. Ham. 2001. Facade orientation as a major design consideration. *Proceedings of ICBEST 2001, International Conference on Building Envelope Systems and Technologies, Ottawa, Canada*, Vol. 1, pp. 45-49.

Gertis, K. 1999, Sind neuere Fassadenentwickelungen bauphysikalisch sinnvoll? Teil 2: Glas-Doppelfassaden (GDF), (in German) Bauphysik 21:54-66.

Haddad, K.H., and A.H. Elmahdy 1998, Comparison of the Monthly Thermal Performance of a Conventional Window and a Supply-Air Window, ASHRAE Transactions, Vol. 104, Part 1B: 1261-1270.

Helbig, S. 1999. Energetische Bewertung von Zuluftfenstern, (in German), Proceedings of the 10th International Symposium for Building Physics, Dresden: 539-548.

Holmes, M.J. 1994. Optimisation of the thermal performance of mechanically and naturally ventilated glazed facades. *Renewable Energy* 5:1091-1098.

Janssens, B. 2003. *Numerieke simulatie van stromingen in de buurt van ventilatiemonden in het kader van de energiehuishouding van een beschermde ruimte/gebouw* (in Dutch), MSc dissertation, Brussel: Royal Military School.

Lang, W. 1998. Zur typology mehrschaliger Gebäudehüllen aus Glass (in German), Detail, nr. 7, pp. 1125-1132.

Lieb, R.-D. 2001. Building physical values of double skin facades. *Proceedings of ICBEST 2001, International Conference on Building Envelope Systems and Technologies, Ottawa, Canada* 1:51-54.

Manz, H., and H. Simmler. 2003. Experimental and numerical study of a mechanically ventilated glass double facade with integrated shading device. *Proceedings of the Research in Building Physics Conference, Leuven, Belgium,* pp. 519-526.

Müller, H., and M. Balowski. 1983. Waste air ventilated windows for offices. *Heizung Luftung Haustechnik*, Vol. 34, n° 10: 412-417.

Oesterle, E., R.-D Lieb, M. Lutz, and W. Heusler. 2001. *Double-Skin Facades—Integrated Planning*. Munich: Prestel.

Park, C.-S. 2003. Occupant responsive optimal control of smart façade systems, Ph.D. dissertation, Georgia Institute of Technology, College of Architecture.

Park, S.-D., H.S. Suh, and S.H. Cho. 1989. The analysis of thermal performance in an airflow window system model. *Proceedings of the ASHRAE/DOE/BTECC/CIBSE Conference, Thermal Performance of the Exterior Envelopes of Buildings IV*, pp. 361-375.

Poirazis, H. 2004. Double skin facades for office buildings—Literature review. Report EBD-R--04/3. Lund: Lund University, Department of Construction and Architecture.

Saelens, D. 2002. Energy performance assessment of multiple-skin facades, Ph.D. dissertation, Leuven: K.U.Leuven, Laboratory of Building Physics.

Saelens, D., S. Roels, and H. Hens. 2004. The inlet temperature as a boundary condition for multiple-skin facade modelling. *Energy and Buildings* 36: 825-835.

Siegel, R., and J.R. Howell. 1992. *Thermal Radiation Heat Transfer*. London: Taylor and Francis.

Tanimoto, J., and K. Kimura. 1997. Simulation study on an airflow window system with an integrated roll screen. *Energy and Buildings*, n° 26:317 - 325.

Ziller, C. 1999. Modellversuche und Berechnungen zur Optimierung der natürlichen Lüftung durch Doppelfassaden (in German), Ph.D. dissertation, Aachen: Shaker Verlag.